Thermal degradation kinetics of in situ prepared PET nanocomposites with acid-treated multi-walled carbon nanotubes

A. A. Vassiliou · K. Chrissafis · D. N. Bikiaris

Abstract A series of PET/acid-treated multi-walled carbon nanotubes (MWCNTs) nanocomposites of varying nanoparticles' concentration were prepared, using the in situ polymerization technique. TEM micrographs verified that the dispersion of the MWCNTs into the PET matrix was homogeneous, while some relatively small aggregates co-existed at higher filler contents. Intrinsic viscosity of the prepared nanocomposites was increased at low MWCNTs contents (up to 0.25 wt%), while at higher contents a gradual reduction was observed. The surface carboxylic groups of acid-treated MWCNTs probably reacted with the hydroxyl end groups of PET, acting as chain extenders at smaller concentrations, while at higher concentrations, on the other hand, led to the formation of branched and cross-linked macromolecules, with reduced apparent molecular weights. From the thermogravimetric curves, it was concluded that the prepared samples exhibited good thermostability, since no remarkable mass loss occurred up to 320 °C (<0.5%). The activation energy (E) of degradation of the studied materials was estimated using the Ozawa, Flynn, and Wall (OFW), Friedman and Kissinger's methods. Pure PET had an $E = 223.5$ kJ/mol, while in the PET/MWCNTs nanocomposites containing up to 1 wt% the E gradually increased, indicating that MWCNTs had a stabilizing effect upon the decomposition of the matrix. Only the sample containing 2 wt% of MWCNTs exhibited a lower E due to the existence of the aforementioned cross-linked macromolecules. The form of the conversion function for all the studied samples obtained by fitting was the mechanism of nth-order auto-catalysis.

Keywords Poly(ethylene terephthalate) · Multi-walled carbon nanotubes · Nanocomposites · Thermal degradation kinetics · Activation energy

Introduction

Poly(ethylene terephthalate) (PET) has been established as a polymeric material of major industrial importance, due to its low cost and high performance (it exhibits high glass transition and melting temperatures), as well as good physical properties. Depending on its processing and thermal history, PET may exist both as an amorphous (transparent) and as a semicrystalline material. It has found a variety of applications, such as in textile fibers, films, bottle containers, food packaging materials, engineering plastics in automobiles, and electronics, etc. Its properties depend mainly on the degree of orientation of the polymer chains and the degree of crystallinity. PET bottles are excellent barrier materials and are widely used with soft carbonated drinks, while in recent years this application has been extended to include alcoholic beverages. The incorporation of organic/inorganic hybrids can result in materials possessing excellent stiffness, strength and gas barrier properties, with far less inorganic content than is commonly used in conventionally filled polymer composites. The enhanced properties usually exhibited by such materials can significantly expand the potential applications of PET [1]. Nanoclays have been the most studied nanofillers

A. A. Vassiliou · D. N. Bikiaris (✉)
Laboratory of Organic Chemical Technology,
Department of Chemistry, Aristotle University of Thessaloniki,
541 24 Thessaloniki, Macedonia, Greece
e-mail: dbic@chem.auth.gr

K. Chrissafis
Solid State Physics Section, Physics Department,
Aristotle University of Thessaloniki, 541 24 Thessaloniki,
Macedonia, Greece

in PET [2–5], while nanocomposites with attapulgite [6], TiO$_2$ [7], SiO$_2$, [8], and calcium carbonate [9] have also been reported. PET/carbon nanotubes composites have recently been studied for their potential application in fuel cells [10, 11], flexible vapour sensors [12], conductive fibers [13] and, furthermore, composite materials with functionalized [14] and acid-treated [15] nanotubes have been prepared.

Apart from mechanical properties and processability, thermal properties and, mainly, resistance to thermal degradation can be enhanced by the addition of appropriate nanoparticles. However, in the case of PET nanocomposites different results have been reported. Yuan et al. found that amino functional groups in amino surfactants decreased the thermal stability of the organoclay and accelerated the degradation behavior of the corresponding PET nanocomposites [16]. Nanocomposites based on clay with a larger amount of hydroxyl groups on the edge of the clay platelets exhibited a much more degradation because the hydroxyl groups acted as Brønsted acidic sites and accelerated the polymer's degradation [17]. The apparent activation energies of PET/fibrous silicates nanocomposites were evaluated using the Kissinger and Flynn–Wall–Ozawa methods [18]. It was suggested that during thermal decomposition in nitrogen the clay can slow down degradation of polymer as a mass-transport protective barrier, but the catalytic effect of the metal derivatives in the clays could accelerate the decomposition behavior of PET. The combination of these two effects determined the final thermal stability of the nanocomposite. However, in an atmosphere of air, the oxidative thermal stability of the PET nanocomposites was significantly superior to that of pure PET. However, opposite were the results by the addition of attapulgite nanoparticles, which could, however, enhance the thermal stability of PET [19]. Furthermore, thermogravimetric analysis suggested that there existed no influence by single wall nanotubes (SWNTs) upon the thermal stability of PET [20]. However, as far as we know, there are no reports about the kinetics of the thermal decomposition behavior of PET with acid-treated multi-walled carbon nanotubes (MWCNTs) nanocomposites.

In the present study, PET/MWCNTs nanocomposites were prepared by in situ polymerization. The objective was to evaluate the effect of the acid-treated MWCNTs upon the thermal degradation of PET nanocomposites, using different kinetic models.

Experimental

Materials

Dimethyl terephthalate (DMT) (99%), anhydrous 1,2-ethanediol (E.G) (99%), antimony trioxide (Sb$_2$O$_3$) (98%),

and triphenylphosphate (TPP) (95%) were obtained from Fluka. Zinc acetate [(CH$_3$CO$_2$)$_2$Zn] (99.99%) was purchased from Aldrich. The MWCNTs [21] used in this study were synthesized by chemical vapor deposition (CVD) and were supplied by Nanothinx (Patra, Greece). They had a diameter between 9 and 20 nm and a length >5 μm. All other materials and solvents used for the analytical methods were of analytical grade.

Acid-treatment of MWCNTs

The pure MWCNTs were functionalized, using the acid treatment method, to introduce reactive groups on their surface. Concentrated nitric acid and sulfuric acid were used for the chemical treatment as described in our previous study [22]. The acid treatment time was 15 min.

In situ prepared PET/MWCNTs nanocomposites

Nanocomposites of poly(ethylene terephthalate) were prepared in situ by the two-stage melt polycondensation of dimethyl terephthalate (DMT) and ethylene glycol (EG) in a glass batch reactor. Appropriate amount of filler was dispersed in EG by ultrasonic vibration (50 W) and intense stirring with a magnetic stirrer (300 rpm) for 10 min prior to polymerization. Zinc acetate was added (1 × 10^{-3} mol/mol DMT) and DMT at a molar ratio of DMT/EG = 1/2.2. The mixture was de-aired and purged with argon three times. Subsequently, it was heated at 190 °C for 1 h, under constant mechanical stirring (500 rpm). The methanol produced by the transesterification reaction was removed from the mixture by distillation and collected in a graduated cylinder. The temperature was raised to 230 °C and the reaction continued for a further 2 h, were the complete removal of the anticipated produced methanol took place.

During the second stage, under an argon atmosphere, the polycondensation catalyst (Sb$_2$O$_3$, 250 ppm) and TPP (0.03 wt% DMT) as thermal stabilizer, dispersed in a small amount of EG, were added in the mixture. TPP prevents side reactions such as etherification and thermal decomposition. Afterwards, vacuum was applied (∼5 Pa) slowly, over a period of 15 min, to avoid excessive foaming and to minimize oligomer sublimation, which is a potential problem during the melt polycondensation. The temperature was raised to 280 °C and the reaction ensued for 2 h. When the polycondensation reaction was completed, the reaction tube was broken to remove the product out of the flask. All polyester samples, after the glass particles were removed with a grinder, were grounded in a mill, sieved, washed with methanol, and dried at 110 °C for 12 h.

Different amounts of MWCNTs were added at the beginning of the transesterification reaction. PET/MWCNT nanocomposites were prepared containing 0.25, 0.5, 1.0, and 2.0 wt% MWCNTs (PET-0.25, PET-0.5, PET-1, and PET-2, respectively).

Intrinsic viscosity measurements

Intrinsic viscosity measurements on the isolated polymers were performed using an Ubbelohde viscometer cap. Ic at 25 °C in phenol/tetrachloroethane 60/40 w/w at a solution concentration of 1 wt%. The solutions were filtered through a disposable membrane filter 0.2 μm (Teflon) prior to the measurement. The intrinsic viscosities $[\eta]$ were calculated using the Solomon–Ciutâ equation [23]:

$$[\eta] = \frac{\sqrt{2 \times (\frac{t}{t_0} - \ln\frac{t}{t_0} - 1)}}{C} \tag{1}$$

where C is the concentration of the solution, t the flow time of the solution and t_0 the flow time of the solvent. Some samples were insoluble in the above solvent mixture. In these samples the insoluble part was removed by filtration and washed extensively first with the solvent mixture and secondly with acetone to remove the solvent. After that it was dried to constant weight by heating at 100 °C under vacuum, in order to measure the insoluble content [24].

Transmission electron microscopy

Electron diffraction (ED) and transmission electron microscopy (TEM) observations were made on ultra thin film samples of the various nanocomposites prepared by an ultra-microtome. These thin films were deposited on copper grids. ED patterns and TEM micrographs were obtained using a JEOL 120 CX microscope operating at 120 kV. In order to avoid the destruction of the films after exposure to the electron irradiation, an adequate sample preparation is required, thus, the thin films were coated with carbon black.

Thermogravimetric analysis

Thermogravimetric analysis (TG) was carried out with a SETARAM SETSYS TG-DTA 1,750 °C. Samples (5.5 ± 0.2 mg) were placed in alumina crucibles. An empty alumina crucible was used as reference. Samples were heated from ambient temperature to 600 °C in a 50 ml/min flow of N_2. Heating rates of 5, 10, 15, and 20 °C/min were used and continuous recordings of sample temperature, sample weight, its first derivative, and heat flow were taken.

Results and discussion

Characterization of the prepared materials

The MWCNTs used in this study were functionalized using chemical oxidation with a mixture of sulfuric and nitric acids [22]. XPS study of the oxidized nanotubes has revealed that the surface is covered with carboxylic (–COOH), carbonyl (−C=O), and hydroxyl (–OH) groups in the approximate proportions of 4:2:1, respectively. These groups increase the chemical reactivity and specificity of the otherwise relatively inert carbon surface. The concentration of the surface acidic groups after the acid treatment was 2.8 meq g^{-1} [22]. The inorganic impurities of the Al–Fe catalyst used in the production of the nanotubes are solubilized by the mixture of inorganic acids and their concentration is reduced with the treatment. The consequences of this oxidative treatment, except for the formation of reactive groups on, mainly, the nanotube's endcaps and at defect sites along the sidewalls, are, simultaneously, the length reduction of the nanotubes into smaller fragments. After 15 min treatment the length of the MWCNTs ranged between 5 and 10 μm.

PET/MWCNTs nanocomposites were prepared in situ during polymerization of PET by the two-stage melt polycondensation method of dimethyl terephthalate (DMT) and ethylene glycol (EG) in a glass batch reactor in the presence of MWCNTs (Fig. 1).

At the first stage of transesterification oligomers are prepared, while methanol is removed as by-product. In
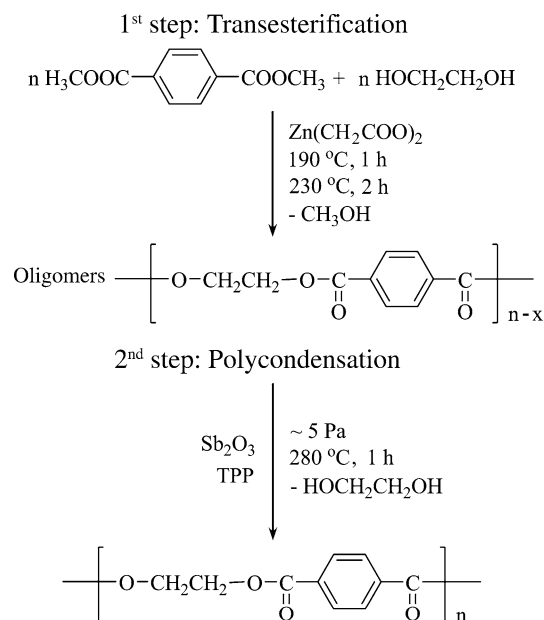

Fig. 1 Synthetic route to PET preparation as well as its nanocomposites with MWCNTs, through the two-step melt polycondensation

order to prepare high molecular weight polyesters, the polycondensation of these oligomers ensued at higher temperature, with the simultaneous application of high vacuum. The intrinsic viscosity of PET that was prepared was 0.57 dL/g. The presence of the MWCNTs in the polymerization mixture affected the reaction, leading to variations of the final intrinsic viscosities of the nanocomposites prepared. As shown in Table 1, the intrinsic viscosity increased at the MWCNT's concentration of 0.25 wt%, and, then, gradually decreased at higher concentrations.

Such a behavior was also observed in previous studies by the addition of SiO_2 nanoparticles, as in the case of poly(ε-caprolactone) [25], prepared by ring opening polymerization, and in poly(butylene succinate) [26], prepared by the two-stage melt polycondensation method. SiO_2 nanoparticles contain surface silanol groups ($\equiv Si–OH$) which, due to their weak acidic nature, can react with the hydroxyl end groups of aliphatic polyesters. It seems plausible that the surface carboxylic groups of acid-treated MWCNTs could also interact with the hydroxyl end groups of PET. In similar nanocomposites containing SiO_2, which can also act as multifunctional additives, it was found that in small amounts SiO_2 nanoparticles could act as chain extender, increasing the molecular weight of the polymer, while at higher contents, due to the extended degree of the aforementioned reaction, branched and crosslinked macromolecules are formed, leading to reduce apparent molecular weights [27, 28]. It is well known that the hydrodynamic dimensions of branched polymers in solution are smaller compared to those of linear polymers with the same molecular weight [29]. Intrinsic viscosity measurements calculate the molecular weight of polymers based on their hydrodynamic size in solution. Therefore, branched polymers appear as having lower molecular weights in comparison to their actual one. This may explain the gradual decrease that observed in molecular weight of the PET samples with concentrations of MWCNTs nanoparticles greater than 0.25 wt%. Another possible contributor to the aforementioned variation of molecular weights was the formation of extensive cross-linkings, resulting in the appearance of an insoluble fraction, as in the case of the sample containing 2 wt% MWCNTs (Table 1).

From TEM micrographs (Fig. 2), it was observed that the dispersion of the MWCNTs into the PET matrix was homogeneous, while at higher concentrations of MWCNTs some small aggregates were also formed. This was due to the extremely high specific area of MWCNTs and the strong interparticle interactions that take place. MWCNTs also influenced the thermal properties of the prepared nanocomposites. From the DSC thermograms the melting point temperatures were calculated. As seen from Table 1, the melting temperatures shifted to lower values by increasing the MWCNTs content. The slight decrease in the melting point might result from the specific interaction between PET and the MWCNTs, since the homogeneous dispersion of MWCNTs affected the formation of PET crystals. It should be mentioned that the formed crystals were of lower perfection compared to those of neat PET and, probably, this was due to the heterogeneous nucleation induced by the MWNTs [30, 31]. Furthermore, the samples containing higher MWCNTs content contained branched and crosslinked macromolecules, which also contributed to the exhibited lower melting points.

Thermogravimetric analysis

Thermal degradation of PET containing different MWCNTs contents was studied by determining its mass loss during heating. In Fig. 3, the mass loss (TG%) and the first derivative of mass loss (DTG) curves of all the studied samples are presented, at a heating rate of 10 °C/min. From the thermogravimetric curves it is obvious that PET and the samples having different MWCNTs content exhibited good thermostability, since no remarkable mass loss occurred up to 320 °C (<0.5%). As seen from the peak of the first

Table 1 Intrinsic viscosity [η] of the prepared PET/MWCNTs nanocomposites

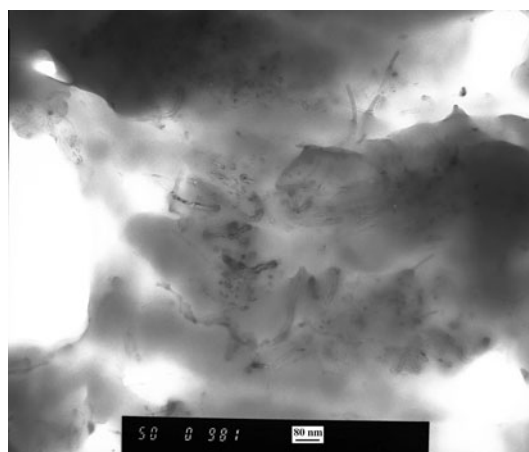| Materials	MWCNTs wt%	[η] dL g^{-1}	Insoluble content/%
PET	0	0.57	–
PET-0.25	0.25	0.63	–
PET-0.5	0.5	0.52	–
PET-1	1	0.49	–
PET-2	2	0.31	2.5

Fig. 2 TEM micrograph of PET/MWCNT nanocomposite containing 1 wt% MWCNTs
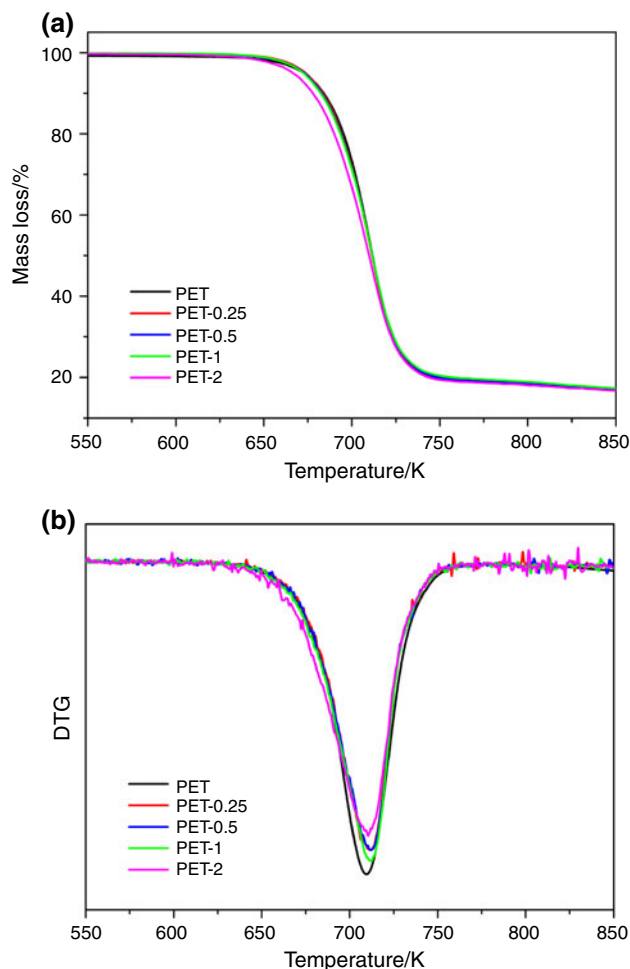
(a)

(b)

Fig. 3 **a** Mass loss (%) versus temperature and **b** first derivative of mass loss (DTG) versus temperature, at a heating rate $\beta = 10$ °C/min for all the studied samples

Fig. 4 Mass loss (%) curves at different heating rates β of PET containing 1 wt% MWCNTs. *1* $\beta = 5$ °C/min, *2* $\beta = 10$ °C/min, *3* $\beta = 15$ °C/min, *4* $\beta = 20$ °C/min

Fig. 5 Derivative mass loss curves at different heating rates β of PET containing 1 wt% MWCNTs. *1* $\beta = 5$ °C/min, *2* $\beta = 10$ °C/min, *3* $\beta = 15$ °C/min, *4* $\beta = 20$ °C/min

derivative, the temperature at which PET decomposition rate was highest was at $T_p = 436.4$ °C, for a heating rate of 10 °C/min. The shape of the mass curve was the same in all samples. In nanocomposites containing up to 1 wt% MWCNTs this temperature was gradually shifted to higher values, up to 439.3 ± 0.5°C, which was an indication that MWCNTs could enhance the thermal stability of the matrix. However, in the sample containing 2 wt% MWCNTs this temperature was shifted to lower values. Since the addition of MWCNTs, as well as that of several other nanoparticles, increased the thermal stability of polymers [32–34], this reduction should be attributed to the presence of extensively branched and crosslinked macromolecules that this sample probably contains.

In order to analyze more thoroughly the degradation mechanism of the PET nanocomposites with MWCNTs, it was important that the kinetic parameters (activation energy E and pre-exponential factor A) and conversion function $f(\alpha)$ were evaluated. The relationship between the
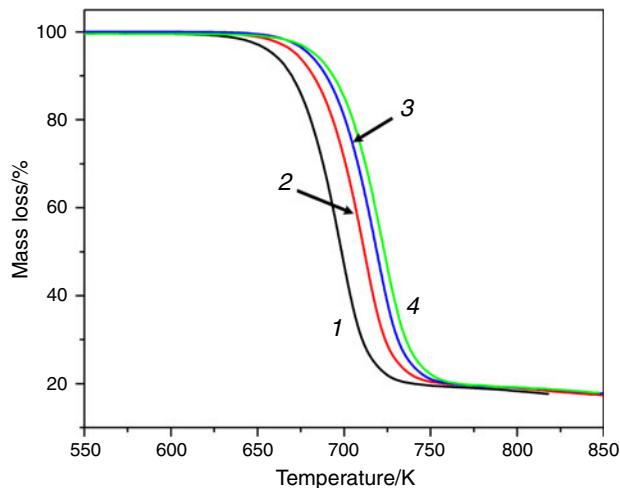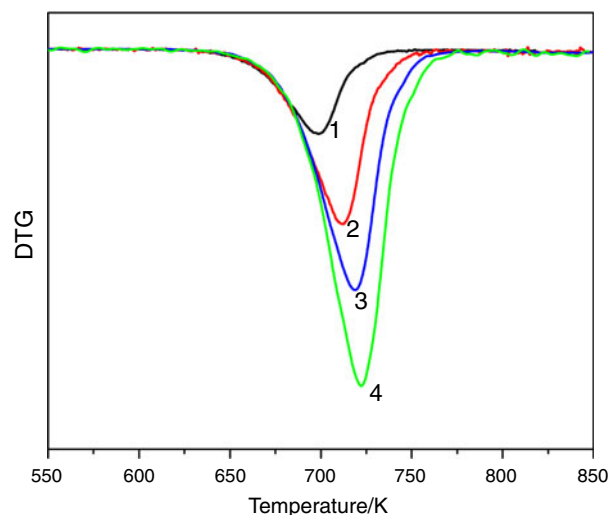
kinetic parameters and conversion (α) can be found using the mass curves recorded in the *TG* dynamic thermograms. The thermogravimetric curves of PET containing 1 wt% MWCNTs, heated in N_2 at different heating rates, are shown in Figs. 4 and 5, at temperatures above the melting point up to 550 °C. It is clear from the *DTG* plots that the peak temperature, T_p, shifted to higher values at increasing heating rates.

The activation energy of degradation of the studied polyester was estimated using the Ozawa, Flynn, and Wall (OFW), Friedman and Kissinger's methods. The isoconversional method of Ozawa, Flynn, and Wall (OFW) [32, 33] is, in fact, a ''model-free'' method which assumes that

the conversion function $f(\alpha)$ does not change with the alteration of the heating rate for all values of the degree of the conversion α. It involves the measuring of the temperatures corresponding to fixed values of α from experiments at different heating rates β. Therefore, plotting $\ln(\beta)$ against $1/T$ according to Eq. 2 in the form of

$$\ln(\beta) = \ln[Af(\alpha)/(d\alpha/dT)] - E/RT \qquad (2)$$

should result in straight lines, the slope of which is directly proportional to the activation energy ($-E/R$). If the determined activation energy is the same for the various values of α, the existence of a single-step reaction can be concluded with certainty. On the contrary, a change in E with increasing degree of conversion is an indication of a complex reaction mechanism that invalidates the separation of variables involved in the OFW analysis [34]. These complications are serious, especially in the case where the total reaction involves competitive reaction mechanisms.

In Fig. 6, the straight lines obtained by fitting the experimental data are presented, for the sample containing 0.5 wt% MWCNTs, with a correlation coefficient greater than 0.999. These lines are nearly parallel ($0.1 < \alpha < 0.9$), thus indicating the applicability of the Ozawa method to our system in the conversion range presented. In Fig. 7 the dependence of the activation energy (E) versus conversion α can be seen, for all the studied samples.

As observed in Fig. 7, the activation energies of the nanocomposites containing up to 1 wt% MWCNTs were higher compared to pure PET. This is an indication that the addition of MWCNTs enhanced the thermal stability of PET. Such behavior is very common in nanocomposites and such thermal stabilization was also reported by the addition of SiO_2 nanoparticles or nanoclays [35–40].
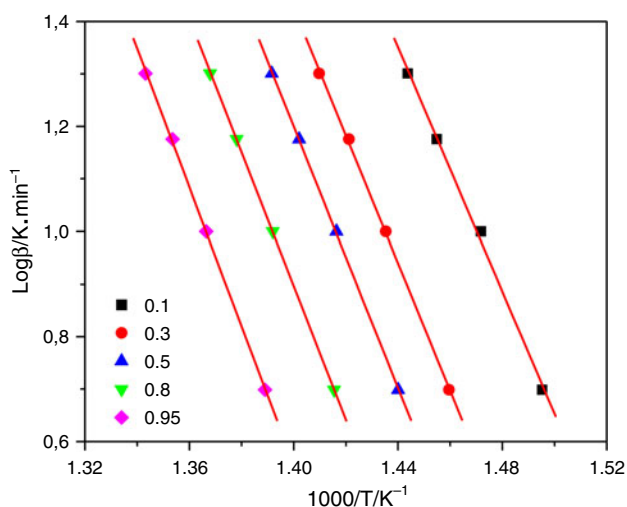

Fig. 6 OFW plots at different degree of the conversion α for PET containing 0.5 wt% MWCNTs
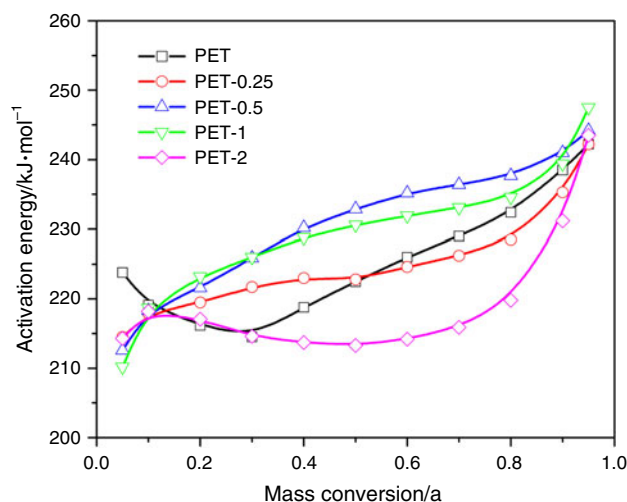
Fig. 7 Dependence of the Activation Energy (E) on the degree of the conversion (α) of the mass loss, as calculated with OFW method for the different samples (*lines drawn for eye guidance*)

However, the sample containing 2 wt% MWCNTs, even though it had the highest content of nanotubes and, thus, the highest prospective thermal stabilization, it had on the contrary the lowest. In all mass conversions the activation rate values were even lower than pure PET. This abnormal behavior should be attributed to the formation of extended branched and crosslinked macromolecules, which reduce thermal stability, in the presence of the MWCNTs.

Friedman [41] proposed the application of the logarithm of the conversion rate $d\alpha/dt$ as a function of the reciprocal temperature, in the form of

$$\ln(d\alpha/dT) = \ln(A/\beta) + \ln f(\alpha) - E/RT \qquad (3)$$

It is obvious from Eq. 2 that if the function $f(\alpha)$ is constant for a particular value of α, then the sum $\ln(f(\alpha)) + \ln A/\beta$ is also constant. By plotting $\ln(d\alpha/dT)_i$ against $1/T_i$, the value of the $-E/R$ for a given value of α can be directly obtained. Using this equation, it is possible to obtain values for E over a wide range of conversions. The results are presented in Fig. 8 and have great similarities with those of Fig. 7. Both methods revealed the same trend of activation energies for the whole conversion range studied. However, comparing the results of the application of the two methods, we observed that the values calculated by the Friedman method were slightly higher than those of the Ozawa method.

The difference in the E value calculated by the two methods can be explained by a systematic error due to improper integration. The method of Friedman employs instantaneous rate values, being therefore very sensitive to experimental noise. In the Ozawa method the equation used is derived assuming constant activation energy, introducing systematic error in the estimation of E in the case that
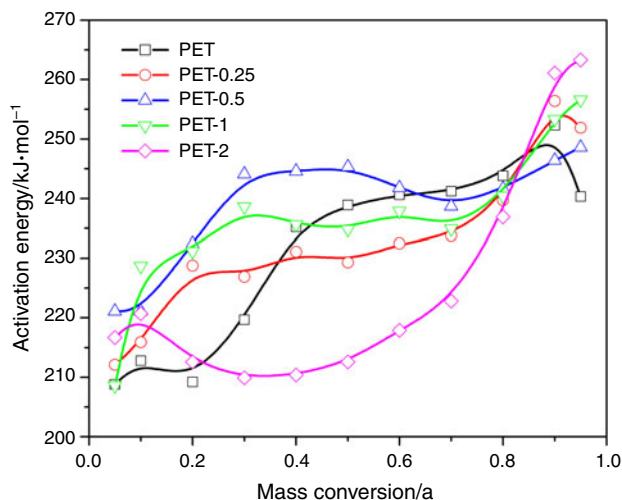
Fig. 8 Dependence of the Activation Energy (E) on the degree of the conversion (α) of the mass loss, as calculated with Friedman's method for the different samples (*lines drawn for eye guidance*)

Fig. 9 Kissinger plots of PET/MWCNTs nanocomposites

E varies with α, error that can be estimated by comparison with the Friedman results [42].

For comparative purpose, we calculated the activation energy calculated using the Kissinger method [43], which has been used in the literature in order to determine activation energy from plots of the logarithm of the heating rate versus the inverse of the temperature at the maximum reaction rate in constant heating rate experiments. The activation energy can be determined by Kissinger method without a precise knowledge of the reaction mechanism, using the following equation:

$$\ln\left(\beta/T_p^2\right) = -E/RT_p + \text{const.} \tag{4}$$

where T_p is the temperature corresponding to the inflection point of the thermal degradation curves, which correspond to the maximum reaction rate. The values of E, for all the studied samples, were obtained from the slope of the $\ln(\beta/T_p^2)$ versus $1/T_p$ plot, with a correlation coefficient greater than 0.995 (Fig. 9).

In order to determine the conversion function $f(\alpha)$, we used a method referred to as the ''model fitting method'' [44, 45]. This method that does not assume the knowledge of E and $f(\alpha)$ in advance, was applied simultaneously on the experimental data taken at the heating rates $\beta = 5, 10, 15,$ and 20 °C/min. For the fitting 16 different kinetic models were used. In Figs. 10 and 11 the results of this fitting for PET and PET containing 0.5 wt% MWCNTs are presented exemplarily. The form of the conversion function, obtained by fitting, was mechanism of nth-order auto-catalysis that is described by the equation $f(a) = (1 - \alpha)^n (1 + K_{cat}X)$. As can be seen, the degradation mechanism in the PET/MWCNTs nanocomposites remained the same, as in the
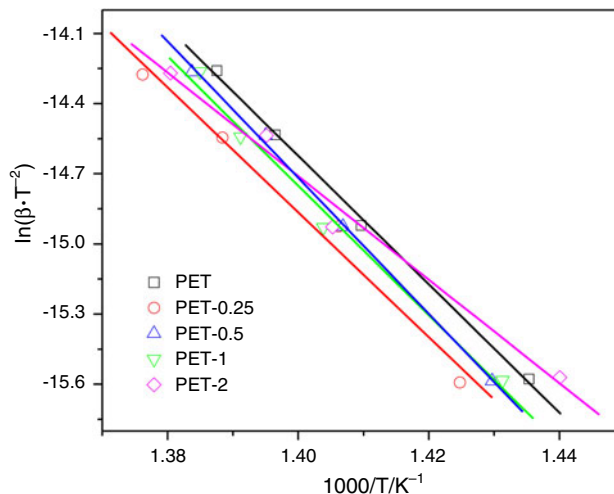

Fig. 10 Fitting and experimental mass (%) curves for all the different heating rates β for PET. *1* $\beta = 5$ °C/min, *2* $\beta = 10$ °C/min, *3* $\beta = 15$ °C/min, *4* $\beta = 20$ °C/min
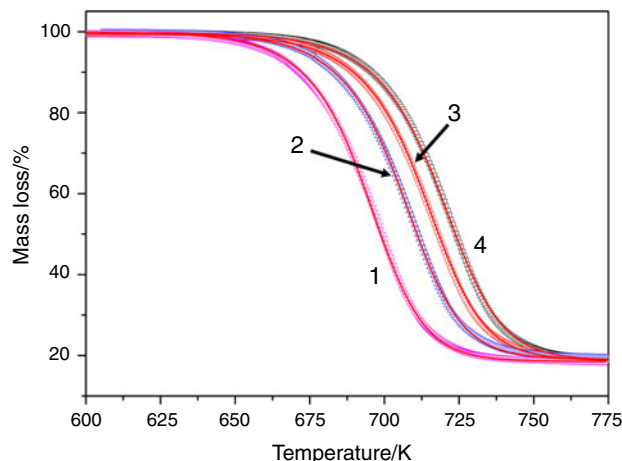

Fig. 11 Fitting and experimental mass loss (%) curves for all the different heating rates β for PET containing 0.5 wt% MWCNTs. *1* $\beta = 5$ °C/min, *2* $\beta = 10$ °C/min, *3* $\beta = 15$ °C/min, *4* $\beta = 20$ °C/min

Table 2 Calculated values of activation energy, pre-exponential factor, and exponent n for all studied samples

Samples	E^a/kJ mol^{-1}	lg$A$	E/kJ mol^{-1}	n	log K_{cat}
PET	228.3	14.05	223.5	1.51	0.73
PET-0.25	230.4	14.26	225.4	1.47	0.55
PET-0.5	242.1	14.88	233.0	1.53	0.53
PET-1	230.0	14.81	231.6	1.49	0.44
PET-2	203.0	13.69	216.0	1.37	0.29

^{a} Calculated values of activation energy using Kissinger's method

case of pure PET. Thus, the addition of the MWCNTs didn't affect the degradation mechanism, but only the activation energies and the decomposition rate. The correlation coefficient was higher than 0.9999. The calculated parameters are shown in Table 2 for all the samples. The values of the activation energy lie between the limits of the calculated values from the Ozawa and Friedman methods and are higher than the calculated ones using Kissinger's method. The fitting to the experimental data was very good for all the range of α. When the value of the activation energy used for fitting was the one calculated by Kissinger's method, the results weren't better compared to the aforementioned ones.

Conclusions

The addition of MWCNTs in situ during polymerization of PET affected most of its properties. MWCNTs acted as multifunctional agents and, as their amount increased, PET macromolecules of lower molecular weight were prepared. This was because branched and crosslinked macromolecules were formed. Thermal decomposition was also improved by the incorporation of MWCNTs into the PET matrix, since the decomposition temperature was shifted to higher values for nanocomposites containing up to 1 wt% MWCNTs. The activation energies for all values of α were determined with the isoconversional methods of Ozawa, Flynn, Wall, and Friedman and it was found that all nanocomposites, except the one containing 2 wt% MWCNTs, exhibited higher activation energies than pure PET. The decomposition mechanism of PET and its nanocomposites with acid-treated MWCNTs was nth-order auto-catalysis and could be described by the equation $f(a) = (1-\alpha)^n(1 + K_{cat}X)$.

References

1. Frounchi M, Dourbash A. Oxygen barrier properties of poly(ethylene terephthalate) nanocomposite films. Macromol Mater Eng. 2009;294(1):68–74.
2. Guan G, Li C, Yuan X, Xiao Y, Liu X, Zhang D. New insight into the crystallization behavior of poly(ethylene terephthalate)/clay nanocomposites. J Polym Sci Polym Phys. 2008;46(21):2380–94.
3. Hwang SY, Lee WD, Lim JS, Park KH, Im SS. Dispersibility of clay and crystallization kinetics for in situ polymerized PET/pristine and modified montmorillonite nanocomposites. J Polym Sci Polym Phys. 2008;46(11):1022–35.
4. de M. Giraldi ALF, Bizarria MTM, Silva AA, Velasco JI, d'Ávila MA, Mei LHI. Effects of extrusion conditions on the properties of recycled poly(ethylene terephthalate)/nanoclay nanocomposites prepared by a twin-screw extruder. J Appl Polym Sci. 2008;108(4):2252–9.
5. Ammala A, Bell C, Dean K. Poly(ethylene terephthalate) clay nanocomposites: Improved dispersion based on an aqueous ionomer. Comp Sci Technol. 2008;68(6):1328–37.
6. Zheng K, Yao X, Chen L, Tian XY. Poly(ethylene terephthalate) clay nanocomposites: improved dispersion based on an aqueous ionomer. J Macromol Sci Phys. 2009;48(2):318–28.
7. Zhu X, Wang B, Chen S, Wang C, Zhang Y, Wang H, et al. Synthesis and non-isothermal crystallization behavior of PET/surface-treated TiO$_2$ nanocomposites. J Macrom Sci Phys. 2008;47(6):1117–29.
8. Yao X, Tian X, Xie D, Zhang X, Zheng K, Xu J, et al. Interface structure of poly(ethylene terephthalate)/silica nanocomposites. Polymer. 2009;50(5):1251–6.
9. Di Lorenzo ML, Errico ME, Avella M. Thermal and morphological characterization of poly(ethylene terephthalate)/calcium carbonate nanocomposites. J Mater Sci. 2002;37(11):2351–8.
10. Wu M, Shaw LL. A novel concept of carbon-filled polymer blends for applications in PEM fuel cell bipolar plates. Int J Hydrogen Energ. 2005;30(4):373–80.
11. Wu M, Shaw LL. On the improved properties of injection-molded, carbon nanotube-filled PET/PVDF blends. J Power Sources. 2004;136(1):37–44.
12. Parikh K, Cattanach K, Rao R, Suh DS, Wu A, Manohar SK. Flexible vapour sensors using single walled carbon nanotubes. Sensor Actuat B Chem. 2006;113(1):55–63.
13. Li Z, Luo G, Wei F, Huang Y. Microstructure of carbon nanotubes/PET conductive composites fibers and their properties. Comput Sci Technol. 2006;66(7–8):1022–9.
14. Lee HJ, Oh SJ, Choi JY, Kim JW, Han J, Tan LS, et al. In Situ synthesis of poly(ethylene terephthalate) (PET) in ethylene glycol containing terephthalic acid and functionalized multiwalled carbon nanotubes (MWNTs) as an approach to MWNT/PET nanocomposites. Chem Mater. 2005;17(20):5057–64.
15. Shin DH, Yoon KH, Kwon OH, Min BG, Hwang CI. Surface resistivity and rheological behaviors of carboxylated multiwall carbon nanotube-filled PET composite film. J Appl Polym Sci. 2006;99(3):900–4.
16. Yuan X, Li C, Guan G, Xiao Y, Zhang D. Thermal stability of surfactants with amino and imido groups in poly(ethylene terephthalate)/clay composites. J Appl Polym Sci. 2008;109(6):4112–20.
17. Xu X, Ding Y, Qian Z, Wang F, Wen B, Zhou H, et al. Degradation of poly(ethylene terephthalate)/clay nanocomposites during melt extrusion: effect of clay catalysis and chain extension. Polym Degrad Stab. 2009;94(1):113–23.
18. Yuan X, Li C, Guan G, Xiao Y, Zhang D. Thermal degradation investigation of poly(ethylene terephthalate)/fibrous silicate nanocomposites. Polym Degrad Stab. 2008;93(2):466–75.

19. Yao X, Tian X, Zhang X, Zheng K, Zheng J, Zhang H, et al. Poly(ethylene terephthalate)/attapulgite nanocomposites: preparation, structure, and properties. J Appl Polym Sci. 2008;110(1): 140–6.
20. Anand KA, Agarwal US, Joseph R. Carbon nanotubes-reinforced PET nanocomposite by melt-compounding. J Appl Polym Sci. 2007;104(5):3090–5.
21. Iijima S. Helical microtubules of graphitic carbon. Nature. 1991;354(6348):56–8.
22. Bikiaris D, Vassiliou A, Chrissafis K, Paraskevopoulos KM, Jannakoudakis A, Docoslis A. Effect of acid treated multi-walled carbon nanotubes on the mechanical, permeability, thermal properties and thermo-oxidative stability of isotactic polypropylene. Polym Degrad Stab. 2008;93(5):952–67.
23. Solomon OF, Ciutâ IZ. Détermination de la viscosité intrinsèque de solutions de polymères par une simple détermination de la viscosité. J Appl Polym Sci. 1962;6(24):683–6.
24. Bikiaris DN, Karayannidis GP. Synthesis and characterisation of branched and partially crosslinked poly(ethylene terephthalate). Polym Int. 2003;52(7):1230–9.
25. Vassiliou A, Papageorgiou GZ, Achilias DS, Bikiaris DN. Non-isothermal crystallisation kinetics of in situ prepared poly(ε-caprolactone)/surface-treated SiO_2 nanocomposites. Macromol Chem Phys. 2007;208(4):364–76.
26. Vassiliou A, Kontopoulou M, Bikiaris DN. Submitted for publication to Macrocoleules.
27. Achilias DS, Bikiaris DN, Karavelidis V, Karayannidis GP. Effect of silica nanoparticles on solid state polymerization of poly(ethylene terephthalate). Eur Polym J. 2008;44(10):3096–107.
28. Bikiaris D, Karavelidis V, Karayannidis G. A new approach to prepare poly(ethylene terephthalate)/silica nanocomposites with increased molecular weight and fully adjustable branching or crosslinking by SSP. Macromol Rapid Commun. 2006;27(15): 1199–205.
29. Zimm BH, Kilb RW. Dynamics of branched polymer molecules in dilute solution. J Polym Sci. 1959;37(131):19–42.
30. Tzavalas S, Mouzakis DE, Drakonakis V, Gregoriou VG. Polyethylene terephthalate-multiwall nanotubes nanocomposites: effect of nanotubes on the conformations, crystallinity and crystallization behavior of PET. J Polym Sci Polym Phys. 2008;46(7): 668–76.
31. Tzavalas S, Drakonakis V, Mouzakis DE, Fisher D, Gregoriou VG. Effect of carboxy-functionalized multiwall nanotubes (MWNT–COOH) on the crystallization and chain conformations of poly(ethyleneterephthalate) PET in PET–MWNT nanocomposites. Macromolecules. 2006;39(26):9150–6.
32. Ozawa T. A new method of analyzing thermogravimetric data. Bull Chem Soc Jpn. 1965;38(11):1881–6.
33. Flynn J, Wall LA. A quick direct method for determination of activation energy from thermogravimetric data. Polym Lett. 1966;4(1966):323–8.
34. Ozawa T. Kinetic analysis of derivative curves in thermal analysis. J Thermal Anal. 1970;2(3):301–24.
35. Chrissafis K, Paraskevopoulos KM, Pavlidou E, Bikiaris D. Thermal degradation mechanism of HDPE nanocomposites containing fumed silica nanoparticles. Thermochim Acta. 2009; 485(1–2):65–71.
36. Chrissafis K, Paraskevopoulos KM, Papageorgiou GZ, Bikiaris D. Thermal and dynamic mechanical behavior of bionanocomposites: fumed silica nanoparticles dispersed in poly(vinyl pyrrolidone), chitosan, and poly(vinyl alcohol). J Appl Polym Sci. 2008;110(3):1739–49.
37. Vassiliou A, Bikiaris D, Chrissafis K, Paraskevopoulos KM, Stavrev SY, Docoslis A. Nanocomposites of isotactic polypropylene with carbon nanoparticles exhibiting enhanced stiffness, thermal stability and gas barrier properties. Comp Sci Technol. 2008;68(3–4):933–43.
38. Araújo EM, Barbosa R, Morais CRS, Soledade LEB, Souza AG, Vieira MQ. Effects of organoclays on the thermal processing of pe/clay nanocomposites. J Therm Anal Calorim. 2007;90(3):841–8.
39. Abate L, Blanco I, Bottino FA, Di Pasquale G, Fabbri E, Orestano A, et al. Kinetic study of the thermal degradation of PS/MMT nanocomposites prepared with imidazolium surfactants. J Therm Anal Calorim. 2008;91(3):681–6.
40. Peila R, Lengvinaite S, Malucelli G, Priola A, Ronchetti S. Modified organophilic montmorillonites/LDPE nanocomposites. J Therm Anal Calorim. 2008;91(1):107–11.
41. Friedman HL. Kinetics of thermal degradation of char-forming plastic from thermogravimetry application to phenolic plastic. J Polym Sci. 1966;4:183–95.
42. Vyazovkin S. Modification of the integral isoconversional method to account for variation in the activation energy. J Comput Chem. 2001;22(2):178–83.
43. Kissinger HE. Reaction kinetics in differential thermal analysis. Anal Chem. 1957;29(11):1702–6.
44. Vyazovkin S, Wight CA. Model-free and model-fitting approaches to kinetic analysis of isothermal and nonisothermal data. Thermochim Acta. 1999;340–341:53–68.
45. Chrissafis K. Kinetics of thermal degradation of polymers: complementary use of isoconversional and model-fitting methods. J Therm Anal Calorim. 2009;95(1):273–83.